ASME 2012 5th Annual Dynamic Systems and Control Conference joint with the
JSME 2012 11th Motion and Vibration Conference
DSCC2012-MOVIC2012
October 17-19, 2012, Fort Lauderdale, Florida, USA

DSCC2012-MOVIC2012-8551

SETPOINT CONTROL OF THE UNCERTAIN ELECTROMAGNETICALLY CONTROLLED OSCILLATOR

Jin Yan, Anthony M. D'Amato, and Dennis S. Bernstein
Department of Aerospace Engineering
University of Michigan
Ann Arbor, MI 48109
Email: yanjin, amdamato, dsbaero @umich.edu

ABSTRACT

We apply an extension of retrospective cost adaptive control (RCAC) to a command-following problem for the uncertain electromagnetically controlled oscillator (ECO). We assume that an estimate of the first Markov parameter of the discretized and linearized plant is known, but RCAC does not require knowledge of the inertia, damping, or stiffness of the plant. RCAC uses a setpoint feedback path and an auxiliary nonlinearity to stabilize the unstable ECO at the commanded equilibria.

INTRODUCTION

Inverse square laws are ubiquitous in physics, for example, in gravitational, electromagnetic, and electrostatic fields. Although the first of these is not (yet) useful for actuation in control, electromagnetic and electrostatic fields are widely used as a means of actuation. When applied over a fixed gap, electromagnetic actuation is easy to manage; this is the basis of rotary motors. When applied over a variable gap, however, electromagnetic actuation can be challenging to work with. The electromagnetically levitated ball is a staple of control labs [1]. However, the restoring force in this case is uniform gravity and thus is independent of displacement. If, however, the restoring force is provided by a stiffness, then the restoring force depends on the displacement, and this dependence leads to extremely challenging dynamics. We call this system the *electromagnetically controlled oscillator* (ECO).

Control of the ECO is considered in [2–7] with applications to linear motors in [8]. As shown in [6] the presence of the stiffness leads to unstable equilibria; in fact, for a linear spring, all equilibria beyond one-third of the initial gap are unstable, and these equilibria become increasingly unstable as the gap increases. In addition, as shown in Figure 3, for each equilibrium current, the ECO has two equilibria; consequently, the domain of attraction and transient response of the adaptive controller can lead to convergence to the "wrong" equilibrium. Another complicating factor is the fact that the applied force is proportional to the square of the current, which introduces a quadratic input nonlinearity [9]. A consequence of this quadratic nonlinearity is the fact that the electromagnetic force is able to pull but not push (assuming a nonmagnetic target mass) and thus the actuation is one-sided. The same observations apply to electrostatic actuation, which is used in MEMS devices [10, 11] and flexible antennas [12, 13].

The goal of the present paper is to develop a control law for the ECO that is applicable to the case in which the mass, damping, and stiffness parameters are uncertain and, in addition, does not use detailed knowledge of the quadratic dependence on current and the inverse-quadratic dependence on the distance between the mass and the electromagnet. This goal is motivated by the realistic situation in which estimates of these parameters are uncertain due to measurement, identification, and calibration errors. Consequently, we do not attempt to invert the input nonlinearities as in [6].

The approach that we take in the present paper is based on retrospective cost adaptive control (RCAC). RCAC is a direct digital control approach that requires minimal modeling information about the plant. RCAC was developed for linear systems, but is extended in [14] to the case of Hammerstein systems with uncertain memoryless input nonlinearities. For the ECO we modify the approach of [14] to account for the fact that, for each equilibrium current, the ECO has two equilibria. Consequently, the domain of attraction and transient response of the adaptive controller can lead to convergence to the "wrong" equilibrium.

To counteract this possibility, we introduce a setpoint feedback path to assist RCAC in reaching the desired equilibrium as the position command increases and thus the mass is moved farther into the unstable region.

The contents of the paper are as follows. In Section II, we present the dynamic model of the ECO and illustrate conditions under which the ECO may have zero, one, or two equilibria. In Section III, we linearize the ECO and analyze its local stability. In Section IV, we construct a feedback controller to have the plant output follow the command signal. We apply an extension of RCAC using auxiliary nonlinearities, and we employ a setpoint feedback path to help RCAC adapt to the new commanded equilibrium. Numerical results are presented in Section V, and conclusions are given in Section VI.

1 Equations of Motion and Equilibria of the ECO

Consider the ECO shown in Figure 1, where m is the mass, i is the manipulated input current to the electromagnet, $c > 0$ is the damping constant, and $k > 0$ is the spring constant. The displacement $q = 0$ corresponds to the position of the mass where the spring is relaxed, and ℓ is the gap between the electromagnet and the relaxed position of the mass. The dynamics of the oscillator are given by

$$m\ddot{q} + c\dot{q} + kq = \frac{\varepsilon i^2}{(\ell - q)^2}, \tag{1}$$

which can be written as

$$\begin{bmatrix} \dot{q} \\ \ddot{q} \end{bmatrix} = A_{\rm c} \begin{bmatrix} q \\ \dot{q} \end{bmatrix} + B_{\rm c} \frac{\varepsilon i^2}{(\ell - q)^2}, \tag{2}$$

where

$$A_{\rm c} \triangleq \begin{bmatrix} 0 & 1 \\ -\frac{k}{m} & -\frac{c}{m} \end{bmatrix}, \quad B_{\rm c} \triangleq \begin{bmatrix} 0 \\ \frac{1}{m} \end{bmatrix}. \tag{3}$$

The parameter ε is a force constant needed to render (1) dimensionally correct. For simplicity, we assume $\varepsilon = 1$ N-m^2/A^2.

Next, let $q_{\rm eq} \in (0, \ell)$ denote the desired equilibrium of the ECO. The corresponding equilibrium current $i_{\rm eq}$ satisfies

$$kq_{\rm eq} = \frac{i_{\rm eq}^2}{(\ell - q_{\rm eq})^2}. \tag{4}$$

Conversely, given a constant current $i_{\rm eq}$, (1) may have zero, one, or two equilibria depending on whether (4) has either zero, one, or two solutions.

Proposition 1.1. The following statements hold:

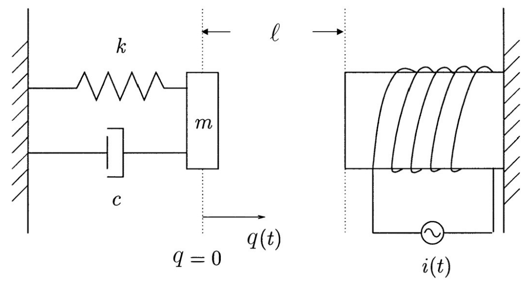

Figure 1. Schematic of the electromagnetically controlled oscillator.

i) If $i_{\rm eq}^2 > \frac{4}{27}k\ell^3$, then (1) has no equilibria.
ii) If $i_{\rm eq}^2 = \frac{4}{27}k\ell^3$, then (1) has a unique equilibrium, which is given by $q_{\rm eq} = \ell/3$.
iii) If $0 < i_{\rm eq}^2 < \frac{4}{27}k\ell^3$, then (1) has two equilibria, namely, $q_{{\rm eq}_1} = \frac{2}{3}\ell(1 - \cos\frac{\alpha}{3})$ and $q_{{\rm eq}_2} = \frac{2}{3}\ell\left[1 + \cos\left(\frac{\alpha}{3} + \frac{\pi}{3}\right)\right]$, where $\alpha \triangleq \cos^{-1}\left(\frac{27 i_{\rm eq}^2}{2k\ell^3} - 1\right)$.

Proof. Let $f_1(q_{\rm eq}) \triangleq kq_{\rm eq}$ and $f_2(q_{\rm eq}) \triangleq \frac{i_{\rm eq}^2}{(\ell - q_{\rm eq})^2}$. Then it follows that $f_1'(q_{\rm eq}) = k$ and $f_2'(q_{\rm eq}) = \frac{2kq}{\ell - q} \in (0, \infty)$. Furthermore, $f_1'(q_{\rm eq}) = f_2'(q_{\rm eq}) = k$ if and only if $q_{\rm eq} = \ell/3$. Therefore, $f_1(q_{\rm eq})$ has no intersection with $f_2(q_{\rm eq})$ if and only if $f_1(\ell/3) < f_2(\ell/3)$, one intersection point if and only if $f_1(\ell/3) = f_2(\ell/3)$, and two intersection points if and only if $f_1(\ell/3) > f_2(\ell/3)$. □

Proposition 1.2. Assume that $0 < i_{\rm eq}^2 < \frac{4}{27}k\ell^3$. Then, $q_{{\rm eq}_1} < \ell/3$ and $q_{{\rm eq}_2} > \ell/3$.

Proof. Since $-1 < \left(\frac{27 i_{\rm eq}^2}{2k\ell^3} - 1\right) < 1$. It follows that $0 < \alpha < \pi$. Hence $\frac{\alpha}{3} \in (0, \frac{\pi}{3})$ and thus $\frac{\alpha}{3} + \frac{\pi}{3} \in (\frac{\pi}{3}, \frac{2\pi}{3})$. Furthermore, $\cos\frac{\alpha}{3} \in (\frac{1}{2}, 1)$ and $\cos\left(\frac{\alpha}{3} + \frac{\pi}{3}\right) \in (-\frac{1}{2}, \frac{1}{2})$. Therefore $q_{{\rm eq}_1} = \frac{2}{3}\ell(1 - \cos\frac{\alpha}{3}) \in (0, \ell/3)$ and $q_{{\rm eq}_2} = \frac{2}{3}\ell\left[1 + \cos\left(\frac{\alpha}{3} + \frac{\pi}{3}\right)\right] \in (\ell/3, \ell)$. □

Proposition 1.1 and Proposition 1.2 are illustrated in Figure 2.

2 Linearization, Local Stability Analysis, and Discretization of the ECO

In this section, we linearize (1) around an equilibrium $q_{\rm eq}$, analyze the local stability, and discretize the linearized plant.

Linearizing (1) around $q = q_{\rm eq}$ yields

$$\begin{bmatrix} \dot{\xi} \\ \ddot{\xi} \end{bmatrix} = A_{\rm l} \begin{bmatrix} \xi \\ \dot{\xi} \end{bmatrix} + B_{\rm l}\delta i, \tag{5}$$

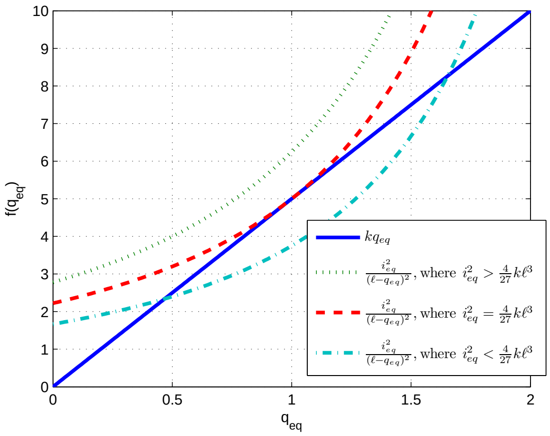

Figure 2. Forced equilibrium position $q_{\rm eq}$ corresponding to various values of $i_{\rm eq}$ for $m = 1$ kg, $\ell = 3$ m, and $k = 5$ N/m. The ECO has no equilibria if and only if $i_{\rm eq}^2 > \frac{4}{27}k\ell^3$, one equilibrium at $q_{\rm eq} = \ell/3 = 1$ m if and only if $i_{\rm eq}^2 = \frac{4}{27}k\ell^3$, and two equilibria if and only if $0 < i_{\rm eq}^2 < \frac{4}{27}k\ell^3$. In the last case, $q_{{\rm eq}_1} < \ell/3$ is asymptotically stable, and $q_{{\rm eq}_2} > \ell/3$ is unstable.

where

$$A_{\rm l} \triangleq \begin{bmatrix} 0 & 1 \\ -\frac{k}{m} + \frac{2i_{\rm eq}^2}{m(\ell-q_{\rm eq})^3} & -\frac{c}{m} \end{bmatrix}, B_{\rm l} \triangleq \begin{bmatrix} 0 \\ \frac{2i_{\rm eq}}{m(\ell-q_{\rm eq})^2} \end{bmatrix}.$$

Next, we define

$$\omega_{\rm n} \triangleq \sqrt{\frac{k}{m}}, \quad \zeta \triangleq \frac{c}{2\sqrt{mk}}, \tag{6}$$

where $\omega_{\rm n} > 0$ denotes the undamped natural frequency of vibration and $\zeta > 0$ denotes the damping ratio. Now $A_{\rm l}$ and $B_{\rm l}$ can be written as

$$A_{\rm l} = \begin{bmatrix} 0 & 1 \\ -\frac{\ell-3q_{\rm eq}}{\ell-q_{\rm eq}}\omega_{\rm n}^2 & -2\zeta\omega_{\rm n} \end{bmatrix}, B_{\rm l} = \begin{bmatrix} 0 \\ \frac{2q_{\rm eq}\omega_{\rm n}^2}{i_{\rm eq}} \end{bmatrix}. \tag{7}$$

The linearized system (5) with $\delta i = 0$ is asymptotically stable if and only if $-\frac{\ell-3q_{\rm eq}}{\ell-q_{\rm eq}}\omega_{\rm n}^2 < 0$, that is,

$$q_{\rm eq} < \ell/3. \tag{8}$$

Figure 3 shows the equilibrium current $i_{\rm eq}$ and the spectral abscissa of $A_{\rm l}$ for each equilibrium of the ECO. Note that $i_{\rm eq}$ decreases as the mass moves farther into the stable region toward the left of $\ell/3$; $i_{\rm eq}$ attains its maximum value $i_{\rm eq} = \sqrt{\frac{4}{27}k\ell^3}$ at $q_{\rm eq} = \ell/3 = 1$ m; and $i_{\rm eq}$ decreases as the mass moves farther into the unstable region to the right of $\ell/3$. Meanwhile, note that the unstable equilibria become increasingly unstable as the mass moves farther to the right of $\ell/3$.

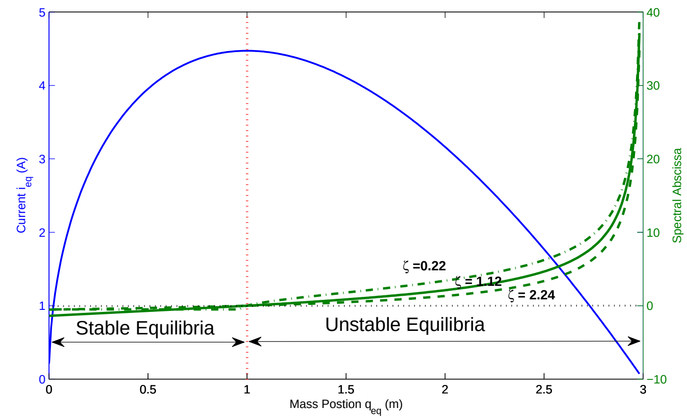

Figure 3. Equilibrium current $i_{\rm eq}$ and spectral abscissa of $A_{\rm l}$ corresponding to each equilibrium of the ECO for $m = 1$ kg, $\ell = 3$ m, $k = 5$ N/m, and $c = 1, 5, 10$ N-s/m respectively. Note that $i_{\rm eq}$ decreases as the mass moves farther into the stable region toward the left of $\ell/3$; $i_{\rm eq}$ attains its maximum value $i_{\rm eq} = \sqrt{\frac{4}{27}k\ell^3}$ at $q_{\rm eq} = \ell/3 = 1$; and $i_{\rm eq}$ decreases as the mass moves farther into the unstable region to the right of $\ell/3$. Meanwhile, the unstable equilibria become increasingly unstable as the mass moves farther to the right of $\ell/3$. Note that by decreasing the damping ratio ζ, the system becomes more unstable.

Next, assuming a zero-order-hold input operator with a sample time of $T_{\rm s}$, we obtain the discretized dynamics

$$x(k+1) = Ax(k) + Bu(k), \tag{9}$$

where $u(k) \triangleq \delta i(k)$. Defining $\gamma \triangleq \frac{\omega_{\rm n}}{2}\left|\zeta^2 - \frac{\ell-3q_{\rm eq}}{\ell-q_{\rm eq}}\right|^{1/2}$, A and B are given by (10) and (11).

3 Command-Following Problem for the ECO

We now consider the ECO command-following problem shown in Figure 4. We apply a feedforward/feedback controller to have the output y follow the command signal r. The goal is to develop an adaptive feedforward/feedback controller that minimizes the command-following error z in the presence of the command signal r with minimal modeling information about the dynamics of the ECO. For the feedforward path, the controller uses a measurement of the command r. For the feedback path, we apply RCAC to the ECO assuming that the state q is available for feedback.

$$A = e^{A_1 T_s} = \begin{cases} e^{-\zeta\omega_n T_s}\begin{bmatrix} \cos\gamma T_s + \zeta\omega_n \sin\gamma T_s & \frac{1}{\gamma}\sin\gamma T_s \\ -\frac{\ell-3q_{eq}}{(\ell-q_{eq})\gamma}\omega_n^2 \sin\gamma T_s & \cos\gamma T_s - \zeta\omega_n \sin\gamma T_s \end{bmatrix}, & \zeta^2 < \frac{\ell-3q_{eq}}{\ell-q_{eq}}, \\ e^{-\zeta\omega_n T_s}\begin{bmatrix} T_s + \zeta\omega_n T_s & bT_s \\ -\frac{\ell-3q_{eq}}{\ell-q_{eq}}\omega_n^2 T_s & T_s - \zeta\omega_n T_s \end{bmatrix}, & \zeta^2 = \frac{\ell-3q_{eq}}{\ell-q_{eq}}, \\ e^{-\zeta\omega_n T_s}\begin{bmatrix} \cosh\gamma T_s + \zeta\omega_n \sinh\gamma T_s & \frac{1}{\gamma}\sinh\gamma T_s \\ -\frac{\ell-3q_{eq}}{(\ell-q_{eq})\gamma}\omega_n^2 \sinh\gamma T_s & \cosh\gamma T_s - \zeta\omega_n \sinh\gamma T_s \end{bmatrix}, & \zeta^2 > \frac{\ell-3q_{eq}}{\ell-q_{eq}}, \end{cases} \tag{10}$$

$$B = \left(\int_0^{T_s} e^{A_1\tau}\mathrm{d}\tau\right)B_1 = \begin{cases} A_1^{-1}(A-I)B_1, & q_{eq} \neq \ell/3, \\ \frac{m}{c}\begin{bmatrix} 0 & \frac{m}{c} \\ 0 & -1 \end{bmatrix}(A-I)B_1 + \begin{bmatrix} \sqrt{3k/\ell}cT_s \\ 0 \end{bmatrix}, & q_{eq} = \ell/3. \end{cases} \tag{11}$$

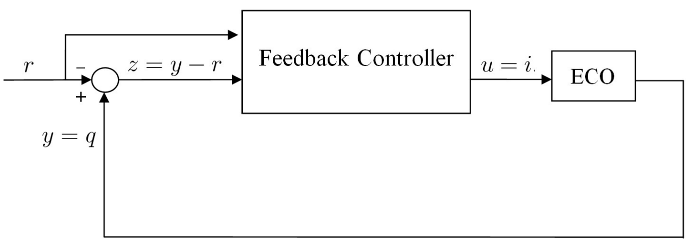

Figure 4. ECO command-following problem.

To account for the nonlinearity of the ECO, the feedforward/feedback controller is constructed as follows. As shown in Figure 5, the RCAC controller uses one auxiliary nonlinearity. The auxiliary nonlinearity $\mathcal{N}_1$ modifies the RCAC controller output u_c to obtain the regressor input u_r. The offset current i_{offset} is determined by the setpoint feedback rule described below.

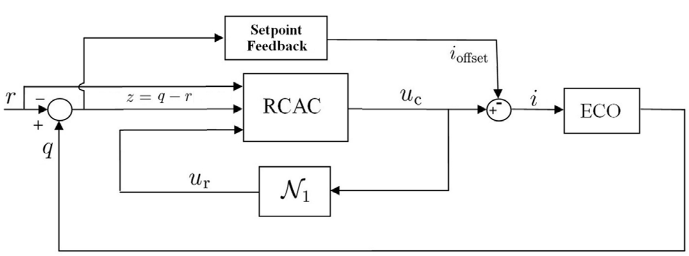

Figure 5. ECO command-following problem with the RCAC adaptive controller and auxiliary nonlinearity $\mathcal{N}_1$. The offset current i_{offset} is determined by the setpoint feedback rule.

3.1 Auxiliary Nonlinearity

Define the saturation function sat_a by

$$\mathrm{sat}_a(x) = \begin{cases} -a, & x < -a, \\ x, & -a \leq x \leq a, \\ a, & x > a, \end{cases} \tag{12}$$

where $a > 0$ is the saturation level.

3.2 Offset Current i_{offset}

Let r be a nondecreasing sequence of step commands, that is, $r(k_1) \leq r(k_2)$ for all $k_1 < k_2$. Then $i_{offset}(k)$ is given by

$$i_{offset}(k) = \begin{cases} 0, & \text{if} \quad 0 < r(k) \leq \ell/3, \\ \rho e^{-\frac{\alpha}{|q(k)-r(k)|^\beta}}, & \text{if} \quad \ell/3 < r(k) < \ell, \end{cases} \tag{13}$$

where $\rho \geq 0$, $\alpha > 0$, $\beta > 0$, and $q(k)$ is the position of the mass at time step k.

As an example, consider $\rho = 1, \alpha = 1, \beta = 1$, and $r(k) = \ell/2$, where $\ell = 3$ m. Figure 6 shows the offset current i_{offset} corresponding to each mass position $q(k)$. Note that the offset current is nonzero except for $q(k) = r(k)$. The offset current increases as the distance between current mass position and commanded mass position increases.

4 Numerical Examples

We now use RCAC with the auxiliary nonlinearity $\mathcal{N}_1$ and the offset current i_{offset} to control the position of the mass. In particular, we consider the command-following problem with the step command $r = q_{eq} \geq \ell/3$.

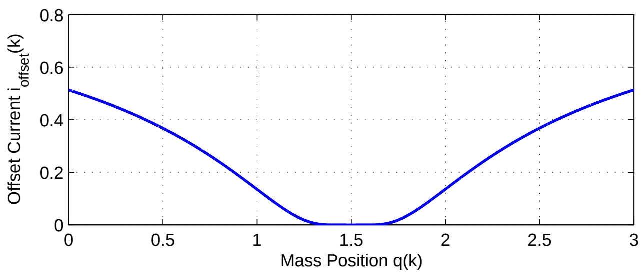

Figure 6. Offset current i_{offset} corresponding to each mass position $q(k)$ for the ECO for $r(k) = 1.5$ m, $\rho = 1, \alpha = 1$, and $\beta = 1$. Note that the offset current is nonzero except for $q(k) = r(k)$. The offset current increases as the distance between current mass position and commanded mass position increases.

The adaptive controller requires an estimate of the first nonzero Markov parameter of the linearized plant (9). This Markov parameter is used to implement the retrospective optimization (26). RCAC generates the control signal u_c, which is added to the offset current i_{offset}.

For simulation we consider $m = 1$ kg, $k = 5$ N/m, $c = 5$ N-s/m, and $\ell = 3$ m with a sample time $T_s = 0.01$ sec. Hence $\omega_n = 2.2361$ rad/s and $\zeta = 1.1180$. First, numerical simulations are performed for the constant command input $q_{eq} = \ell/3 = 1.0$ m. The first nonzero Markov parameter of (5) is $H_1(q_{eq}) \stackrel{\triangle}{=} CB$, where B is defined in (11) and $C \stackrel{\triangle}{=} \begin{bmatrix} 1 & 0 \end{bmatrix}$. We choose $H_1(q_{eq}) = H_1(1) = 1.0996 \times 10^{-4}$ m/A. Figure 7 shows the dependence of H_1 on the equilibria of the ECO. We initialize the control gains to zero, that is, $\theta(0) = 0$, and we choose the controller order $n_c = 8$ and the covariance matrix $P(0) = 10^{-9} I_{3n_c}$. Furthermore, since the linearized model is minimum phase, we choose the regularization $\eta = 0$. Finally, we set $\rho = 0$ so that $i_{\text{offset}} = 0$, and we do not use a forgetting factor in the adaptive controller, that is, $\lambda = 1$. Figure 8 shows that the controller stabilizes the plant and follows the command input. Figure 9 shows the time history of the control input u_c. It follows from Proposition 1.1 that the steady-state value of the current $i = u_c$ is the maximum current such that (1) has an equilibrium.

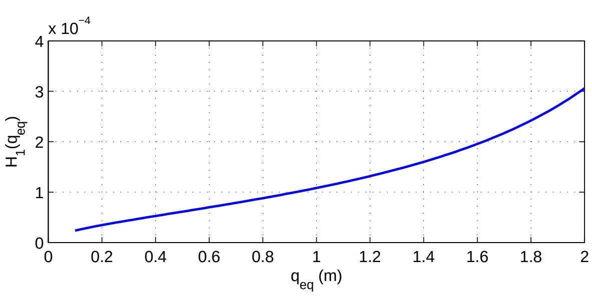

Figure 7. H_1 corresponds to each equilibrium of the ECO for $m = 1$ kg, $\ell = 3$ m, $c = 5$ N-s/m, and $k = 5$ N/m.

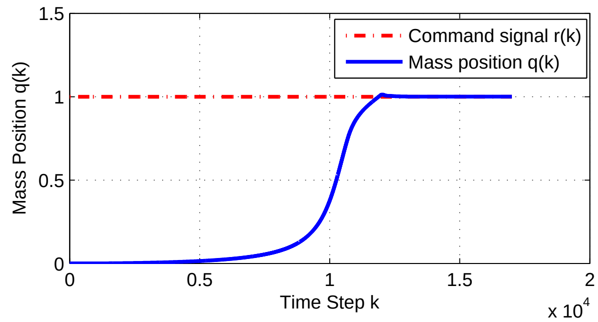

Figure 8. Position of the mass with the step command $r(k) = \mathbf{1}(k)$ for $m = 1$ kg, $\ell = 3$ m, $c = 5$ N-s/m, and $k = 5$ N/m. In this simulation, $\hat{H}_1(1) = H_1(1)$. Since $r(k) = \mathbf{1}(k) = \ell/3$, it follows that $i_{\text{offset}} = 0$.

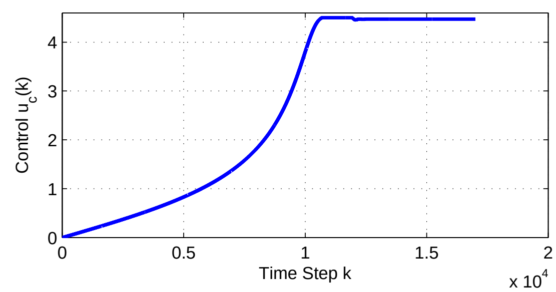

Figure 9. Time history of the control input u_c corresponding to the closed-loop response shown in Figure 8. In this case, $i_{\text{offset}} = 0$.

Next, we do not assume that $H_1(1)$ is known exactly [15]. Figure 10 shows the position of the mass with various estimates $\hat{H}_1(1)$ of $H_1(1)$. The RCAC controller is able to stabilize the plant and follow the step command with erroneous estimates of $H_1(1)$. However, the best overall performance for both the transient response and the convergent time is obtained for $\hat{H}_1(1) = H_1(1)$.

Now, we implement the adaptive controller with a nondecreasing sequence of setpoint commands as shown by Figure 11. To do this, we set i_{offset} based on (6) when $r(k) > \ell/3$. In particular, we choose $\rho = 1$, $\alpha = 1, \beta = 1$, $\hat{H}_1(1) = H_1(1)$, $n_c = 8$, and initialize the control gains to zero. Figure 11 shows that the control algorithm is able to stabilize the system up to $q_{eq} = 1.79$. Figure 12(a) shows the time history of the current offset i_{offset}, and Figure 12(b) shows the time history of the control input u_c from the RCAC.

Finally, we reduce the damping coefficient so that $c = 4$ N-s/m, and thus the ECO is underdamped with $\zeta = 0.8944$. Following the same procedure, and using the same parameters for initializing RCAC, Figure 13 shows that RCAC is able to stabilize the underdamped system up to $q_{eq} = 1.79$. Figure 14(a) shows the time history of the current offset i_{offset}, and Figure 14(b) shows the time history of the control input u_c from RCAC. Note that, in this case, the transient response for the open-loop underdamped ECO system is worse than the response in the open-loop overdamped case. Figure 15 shows the largest distance the mass

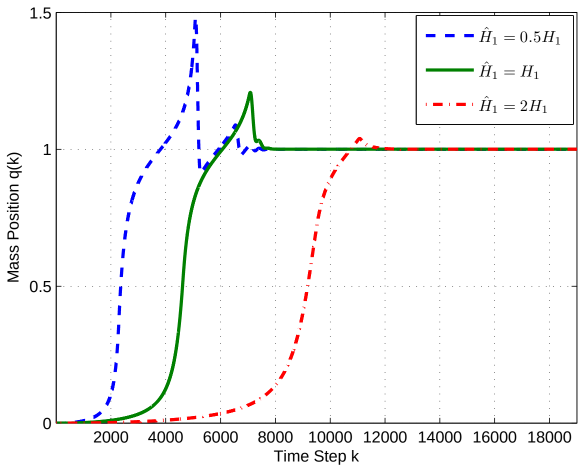

Figure 10. Position of the mass with the step command $r(k) = \mathbf{1}(k)$ with various estimates $\hat{H}_1(1)$ of $H_1(1)$ for $m = 1$ kg, $\ell = 3$ m, $c = 5$ N-s/m, and $k = 5$ N/m. The controller is able to stabilize the plant and follow the step commands in all cases. However, the accuracy of $\hat{H}_1(1)$ affects the transient response. In this case, $i_{\text{offset}} = 0$.

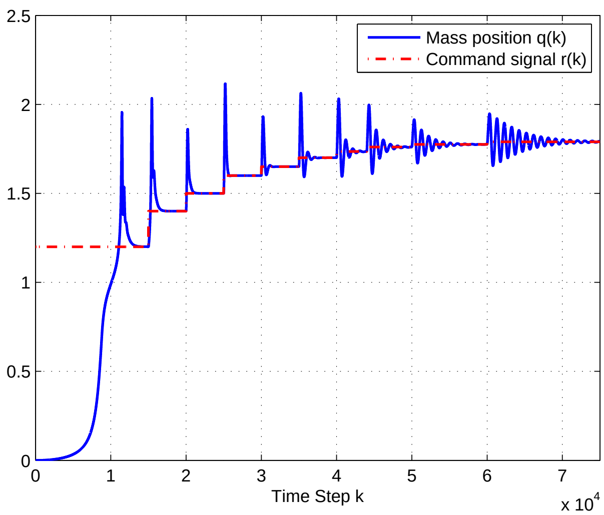

Figure 11. Position of the mass with a nondecreasing sequence of step commands for $m = 1$ kg, $\ell = 3$ m, $c = 5$ N-s/m, and $k = 5$ N/m, where $\zeta = 1.1180$. In order to stabilize the mass close to the electromagnet, the command signal is a nondecreasing sequence of step commands, which is shown as the red dash line. Note that all equilibria greater than $q_{\text{eq}} = 1$ are open-loop unstable. In this simulation, we choose $\hat{H}_1 = H(1)$.

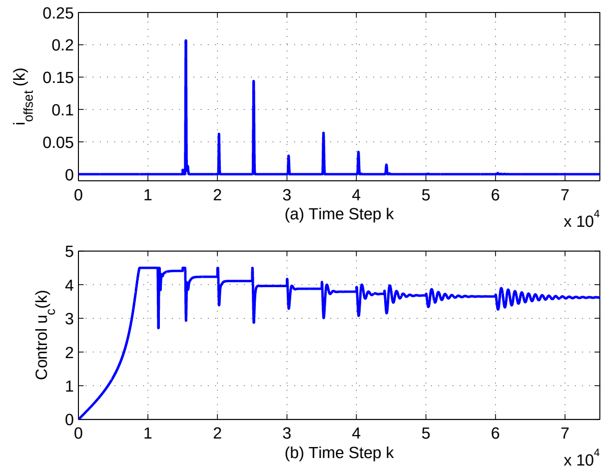

Figure 12. Current offset i_{offset} (a) and control input u_{c} (b) corresponding to the closed-loop response shown in Figure 11.

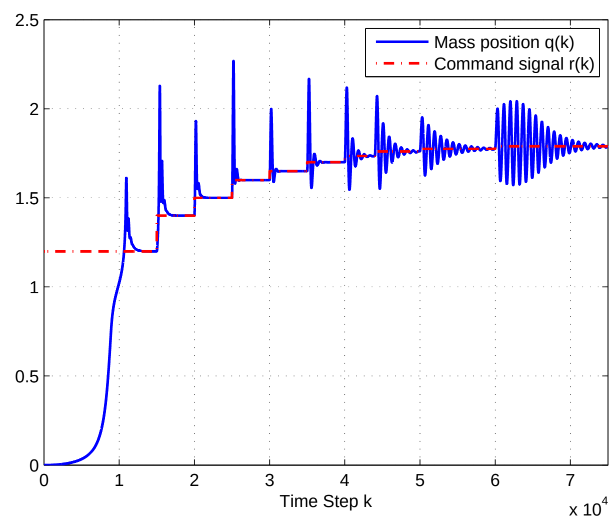

Figure 13. Position of the mass with a nondecreasing sequence of step commands for $m = 1$ kg, $\ell = 3$ m, $c = 4$ N-s/m, and $k = 5$ N/m, where $\zeta = 0.8944$. In order to stabilize the mass close to the electromagnet, the command signal is a nondecreasing sequence of step commands, which is shown as the red dash line. Note that we choose $\hat{H}_1 = H(1)$, and all equilibria greater than $q_{\text{eq}} = 1$ are open-loop unstable. In this case, which is underdamped, the transient response is worse than the response in Figure 11.

can be moved by the feedforward/feedback controller versus the open-loop damping ratio of the ECO system. Note that, in all those cases, we choose $\hat{H}_1 = H(1)$.

Finally, to demonstrate the potential benefits of scheduling the Markov parameters as a function of q_{eq}, we consider the same example shown in Figure 11. Since the Markov parameter increases as the mass moves farther into the unstable region (in Figure 7), we thus let $\hat{H}_1 = H(1)$ for $q_{\text{eq}} \in (0, 1.7)$ and $\hat{H}_1 = 1.2H(1)$ for $q_{\text{eq}} \geq 1.7$. Figure 16 shows that RCAC is able to stabilize the system up to $q_{\text{eq}} = 1.815$.

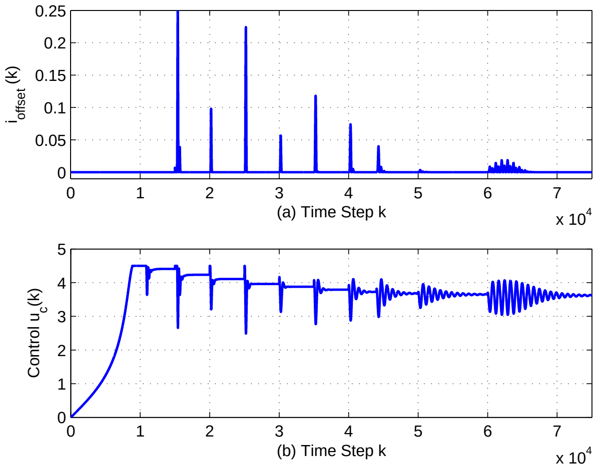

Figure 14. Current offset i_{offset} (a) and control input u_{c} (b) corresponding to the closed-loop response shown in Figure 13.

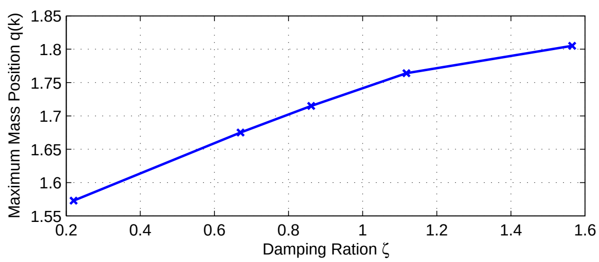

Figure 15. Largest distance that RCAC is able to move the mass for various open-loop damping ratios of the ECO. In all cases, we choose $\hat{H}_1 = H(1)$, that is, the Markov parameter for the ECO linearized at $q = 1$ for the simulation.

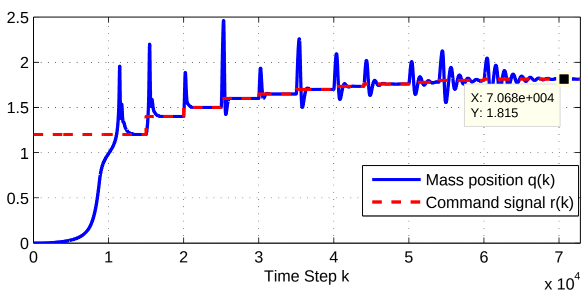

Figure 16. Position of the mass with a nondecreasing sequence of step commands for $m = 1$ kg, $\ell = 3$ m, $c = 5$ N-s/m, and $k = 5$ N/m, where $\zeta = 1.1180$. Note that all equilibria greater than $q_{\text{eq}} = 1$ are open-loop unstable. In this simulation, we let $\hat{H}_1 = H(1)$ for $q_{\text{eq}} \in (0, 1.7)$ and $\hat{H}_1 = 1.2H(1)$ for $q_{\text{eq}} \geq 1.7$. RCAC is able to stabilize the system up to $q_{\text{eq}} = 1.815$.

5 Conclusions

In this paper, we considered a command-following problem for the electromagnetically controller oscillator (ECO). RCAC was used with limited modeling information, namely, an estimate of the first nonzero Markov parameter of the linearized system. To handle the effect of the nonlinearities and the unstable region of the ECO, RCAC was augmented by an auxiliary nonlinearity. An equilibrium feedback path was also used to assist RCAC in reaching the desired unstable equilibrium. Future research will focus on the effect of noise and sample rate as well as the potential benefits of scheduling the Markov parameters as a function of q_{eq}.

REFERENCES

[1] Lundberg, K. H., Lilienkamp, K. A., and Marsden, G., 2004. "Low-cost magnetic levitation project kits". *IEEE Contr. Sys. Mag.,* **24**, pp. 65–69.

[2] Hong, J., Cummings, I. A., Washabaugh, P. D., and Bernstein, D. S., 1997. "Stabilization of a mass and spring system with electromagnetic actuation". *Proc. Conf. Contr. Appl.*, October, pp. 189–194.

[3] Hong, J., Cummings, I. A., Bernstein, D. S., and Washabaugh, P. D., 1998. "Stabilization of an electromagnetically controlled oscillator". *Proc. Amer. Contr. Conf.*, June, pp. 2775–2779.

[4] Sane, H. S., and Bernstein, D. S., 2002. "Robust nonlinear control of the electromagnetically controlled oscillator". *Proc. Amer. Contr. Conf.*, May, pp. 809–814.

[5] Miller, R. H., Kolmanovsky, I., Gilbert, E. G., and Washabaugh, P. D., 2000. "Control of Constrained Nonlinear Systems: A Case Study". *IEEE Contr. Sys. Mag.,* **19**, pp. 23–32.

[6] Sane, H., and Bernstein, D. S., 2003. "Asymptotic Disturbance Rejection for Hammerstein Positive Real Systems". *IEEE Trans. Contr. Sys. Tech.,* **11**, pp. 364–374.

[7] Su, J., Yang, H., Fay, P., Porod, W., and Bernstein, G. H., 2010. "A surface micromachined offset-drive method to extend the electrostatic travel range". *Journal of Micromechanics and Microengineering,* **20**, pp. 1–10.

[8] Cairano, S. D., Bemporad, A., Kolmanovsky, I., and Hrovat, D., 2007. "Model predictive control of magnetically actuated mass spring dampers for automotive applications". *Int. J. Contr.,* **80**(11), pp. 1701–1716.

[9] Zhong, J., Cheng, D., and Hu, X., 2008. "Constructive stabilization for quadratic input nonlinear systems". *Automatica,* **44**, pp. 1996–2005.

[10] Maithripala, D. H. S., Berg, J. M., and Dayawansa, W. P., 2003. "A virtual velocity sensor for improved transient performance of electrostatically actuated mems". In Proc. ASME Ing. Mech. Eng. Congress Expos., pp. 1–5. IMECE2003-42451.

[11] Sane, H. S., 2006. "Energy-based control for mems with one-sided actuation". *Proc. Amer. Contr. Conf.*, June, pp. 1209–1214.

[12] Lang, J. H., and Staelin, D. H., 1982. "Electrostatically figured reflecting membrane antennas for satellites". *IEEE*

Trans. Autom. Contr., **27**, pp. 666–670.
[13] Mihora, D. J., and Redmond, P. J., 1980. "Electrostatically formed antennas". *Journal of Spacecraft,* **17**, pp. 465–475.
[14] Yan, J., D'Amato, A. M., Sumer, E. D., Hoagg, J. B., and Bernstein, D. S., 2012. "Adaptive control of uncertain hammerstein systems using auxiliary nonlinearities". *submitted to IEEE Conf. Dec. Contr*, December.
[15] D'Amato, A. M., Sumer, E. D., and Bernstein, D. S., 2011. "Frequency-domain stability analysis of retrospective-cost adaptive control for systems with unknown nonminimum-phase zeros". *Proc. IEEE Conf. Dec. Contr.*, December, pp. 1098–1103.
[16] Hoagg, J. B., and Bernstein, D. S., 2010. "Retrospective cost adaptive control for nonminimum-phase discrete-time systems part 1: The ideal controller and error system; part 2: The adaptive controller and stability analysis". *Proc. IEEE Conf. Dec. Contr.*, December, pp. 893–904.
[17] Hoagg, J. B., Santillo, M. A., and Bernstein, D. S., 2008. "Discrete-time adaptive command following and disturbance rejection for minimum phase systems with unknown exogenous dynamics". *IEEE Trans. Autom. Contr.,* **53**, pp. 912–928.
[18] Santillo, M. A., and Bernstein, D. S., 2010. "Adaptive control based on retrospective cost optimization". *AIAA J. Guid. Contr. Dyn.,* **33**, pp. 289–304.

Appendix: Review RCAC

In this section, we review the cumulative retrospective cost adaptive controller presented in [15]. First, consider the MIMO discrete-time system

$$x(k+1) = Ax(k) + Bu(k), \tag{14}$$
$$y_0(k) = E_1 x(k), \tag{15}$$
$$z(k) = r(k) - y_0(k), \tag{16}$$

where $x(k) \in \mathbb{R}^n$, $z(k) \in \mathbb{R}^{l_z}$, $u(k) \in \mathbb{R}^{l_u}$, $r(k) \in \mathbb{R}^{l_w}$, and $k \geq 0$. Our goal is to develop an adaptive output feedback controller that minimizes the command-following error z in the presence of the command signal r with minimal modeling information about the dynamics and r.

We represent(14) and (16) as the time-series model from u to z given by

$$z(k) = E_1 A^m x(k-m) - E_0 r(k) + \bar{H}\bar{U}(k-1), \tag{17}$$

where $k > m$

$$\bar{H} \stackrel{\triangle}{=} \begin{bmatrix} H_1 & \cdots & H_m \end{bmatrix} \in \mathbb{R}^{l_z \times m l_u}$$

the Markov parameter $H_i \stackrel{\triangle}{=} E_1 A^{i-1} B$, and

$$\bar{U}(k-1) \stackrel{\triangle}{=} \begin{bmatrix} u(k-1) \\ \vdots \\ u(k-m) \end{bmatrix}$$

Next, we present an adaptive control algorithm for the general control problem represented by (14)–(16). The control $u(k)$ is given by the strictly proper time-series controller of order n_c

$$u(k) = \sum_{i=1}^{n_c} M_i(k) u(k-i) + \sum_{i=1}^{n_c} N_i(k) z(k-i), \tag{18}$$

where, for all $i = 1, \ldots, n_c$, $M_i(k) \in \mathbb{R}^{l_u \times l_u}$ and $N_i(k) \in \mathbb{R}^{l_u \times l_z}$. The control (18) can be expressed as

$$u(k) = \theta(k)\phi(k-1), \tag{19}$$

where

$$\theta(k) \stackrel{\triangle}{=} \begin{bmatrix} M_1(k) & \cdots & M_{n_c}(k) & N_1(k) & \cdots & N_{n_c}(k) \end{bmatrix} \in \mathbb{R}^{l_u \times n_c(l_u + l_z)} \tag{20}$$

and

$$\phi(k-1) \stackrel{\triangle}{=} \begin{bmatrix} u(k-1) \\ \vdots \\ u(k-n_c) \\ z(k-1) \\ \vdots \\ z(k-n_c) \end{bmatrix} \in \mathbb{R}^{n_c(l_u + l_y)}.$$

Next, we define the the *surrogate performance*

$$\hat{z}(k-k_j) \stackrel{\triangle}{=} \mathcal{S}_j(k-k_j) + \mathcal{H}_j \hat{U}_j(k-k_j-1), \tag{21}$$

where $\mathcal{S}(k) \stackrel{\triangle}{=} E_1 A^m x(k-m) - E_0 r(k) + \mathcal{H}' U'(k-1)$, and the past controls $U_j(k-k_j-1)$ are replaced by the surrogate controls $\hat{U}_j(k-k_j-1)$. Now, we express *extended surrogate performance* as

$$\hat{Z}(k) \triangleq \begin{bmatrix} \hat{z}(k-k_1) \\ \vdots \\ \hat{z}(k-k_s) \end{bmatrix} \in \mathbb{R}^{sl_z}$$

and thus is given by

$$\hat{Z}(k) = \tilde{\mathcal{S}}(k) + \tilde{\mathcal{H}}\hat{\tilde{U}}(k-1), \tag{22}$$

where the components of $\hat{\tilde{U}}(k-1) \in \mathbb{R}^{l_{\tilde{U}}}$ are the components of $\hat{U}_1(k-k_1-1), \ldots, \hat{U}_s(k-k_s-1)$ ordered in the same way as the components of $\tilde{U}(k-1)$. Hence

$$\hat{Z}(k) = Z(k) - \tilde{\mathcal{H}}\tilde{U}(k-1) + \tilde{\mathcal{H}}\hat{\tilde{U}}(k-1). \tag{23}$$

Finally, we define the *retrospective cost function*

$$J(\hat{\tilde{U}}(k-1), k) \triangleq \hat{Z}^{\mathrm{T}}(k)R(k)\hat{Z}(k), \tag{24}$$

where $R(k) \in \mathbb{R}^{l_z s \times l_z s}$ is a positive-definite performance weighting. To ensure that (24) has a global minimizer, we consider the regularized cost

$$\bar{J}(\hat{\tilde{U}}(k-1), k) \triangleq \hat{Z}^{\mathrm{T}}(k)R(k)\hat{Z}(k) + \eta(k)\hat{\tilde{U}}^{\mathrm{T}}(k-1)\hat{\tilde{U}}(k-1), \tag{25}$$

where $\eta(k) \geq 0$. where $\eta(k) \geq 0$. Substituting (23) into (25) yields

$$\begin{aligned}\bar{J}(\hat{\tilde{U}}(k-1), k) = \hat{\tilde{U}}(k-1)^{\mathrm{T}}\mathcal{A}(k)\hat{\tilde{U}}(k-1) + \mathcal{B}(k)\hat{\tilde{U}}(k-1) \\ + \mathcal{C}(k),\end{aligned}$$

where

$$\begin{aligned}\mathcal{A}(k) &\triangleq \tilde{\mathcal{H}}^{\mathrm{T}}R(k)\tilde{\mathcal{H}} + \eta(k)I_{l_{\tilde{U}}}, \\ \mathcal{B}(k) &\triangleq 2\tilde{\mathcal{H}}^{\mathrm{T}}R(k)[Z(k) - \tilde{\mathcal{H}}\tilde{U}(k-1)], \\ \mathcal{C}(k) &\triangleq Z^{\mathrm{T}}(k)R(k)Z(k) - 2Z^{\mathrm{T}}(k)R(k)\tilde{\mathcal{H}}\tilde{U}(k-1) \\ &\quad + \tilde{U}^{\mathrm{T}}(k-1)\tilde{\mathcal{H}}^{\mathrm{T}}R(k)\tilde{\mathcal{H}}\tilde{U}(k-1).\end{aligned}$$

If either $\tilde{\mathcal{H}}$ has full column rank or $\eta(k) > 0$, then $\mathcal{A}(k)$ is positive definite. In this case, $\bar{J}(\hat{\tilde{U}}(k-1), k)$ has the unique global minimizer

$$\hat{\tilde{U}}(k-1) = -\frac{1}{2}\mathcal{A}^{-1}(k)\mathcal{B}(k). \tag{26}$$

Next, let $d > 0$ be such that $\tilde{U}(k-1)$ contains $u(k-d)$ and define the retrospective cost function

$$\begin{aligned}J_{\mathrm{R}}(\theta(k)) \triangleq \sum_{i=d+1}^{k} \lambda^{k-i}\|\phi^{\mathrm{T}}(i-d-1)\theta^{\mathrm{T}}(k) - \hat{u}^{\mathrm{T}}(i-d)\|^2 \\ + \lambda^k(\theta(k) - \theta(0))P^{-1}(0)(\theta(k) - \theta(0))^{\mathrm{T}},\end{aligned} \tag{27}$$

where $\|\cdot\|$ is the Euclidean norm, and $\lambda \in (0,1]$ is the forgetting factor. Minimizing (27) yields

$$\begin{aligned}\theta^{\mathrm{T}}(k) = \theta^{\mathrm{T}}(k-1) + P(k-1)\phi(k-d-1) \\ \cdot[\phi^{\mathrm{T}}(k-d)P(k-1)\phi(k-d-1) + \lambda(k)]^{-1} \\ \cdot[\phi^{\mathrm{T}}(k-d-1)\theta^{\mathrm{T}}(k-1) - \hat{u}^{\mathrm{T}}(k-d)],\end{aligned}$$

The error covariance is updated by

$$\begin{aligned}P(k) = \lambda^{-1}P(k-1) \\ -\lambda^{-1}P(k-1)\phi(k-d-1) \\ \cdot[\phi^{\mathrm{T}}(k-d-1)P(k-1)\phi(k-d) + \lambda(k)]^{-1} \\ \cdot\phi^{\mathrm{T}}(k-d-1)P(k-1).\end{aligned}$$

We initialize the error covariance matrix as $P(0) = \alpha I$, where $\alpha > 0$. For other choices of the parameters and the stability analysis, see [16–18].